WITHIN-FIELD VARIABILITY IN GRANULAR MATRIX SENSOR DATA AND ITS IMPLICATIONS FOR IRRIGATION SCHEDULING

T. Lo, H. C. Pringle, III, D. R. Rudnick, G. Bai, L. J. Krutz, D. M. Gholson, X. Qiao

Beyond 2020, VISION OF THE FUTURE Collection
Research

HIGHLIGHTS

- Within-field variability was larger for individual depths than for the profile average across multiple depths.
- Distributions of the profile average were approximately normal, with increasing variances as the soil was drying.
- Probability theory was applied to quantify the effect of sensor set number on irrigation scheduling.
- The benefit of additional sensors sets may decrease for longer irrigation cycles and for more heterogeneous fields.

ABSTRACT. *Even when located within the same field, multiple units of the same soil moisture sensor rarely report identical values. Such within-field variability in soil moisture sensor data is caused by natural and manmade spatial heterogeneity and by inconsistencies in sensor construction and installation. To better describe this variability, daily soil water tension values from 14 to 23 sets of granular matrix sensors during the middle part of four soybean site-years in the Mississippi Delta were analyzed. The soil water tension data were found to follow approximately normal distributions, to exhibit moderately high temporal rank stability, and to show strong positive correlation between mean and variance. Based on these observations and the existing literature, a probabilistic conceptual framework was proposed for interpreting within-field variability in granular matrix sensor data. This framework was then applied to investigate the impact of sensor set number (i.e., number of replicates) and irrigation triggering threshold on the scheduling of single-day and multi-day irrigation cycles. If a producer's primary goal of irrigation scheduling is to keep soil water adequate in a particular fraction of land on average, the potential benefit from increasing sensor set number may be smaller than traditionally expected. Improvement, expansion, and validation of this probabilistic framework are welcomed for developing a practical and robust approach to selecting the sensor set number and the irrigation triggering threshold for diverse soil moisture sensor types in diverse contexts.*

Keywords. *Irrigation scheduling, Probability, Sensors, Soil moisture, Soil water tension, Variability, Watermark.*

Much of the soil moisture sensor literature has been dedicated to evaluating and improving sensor calibrations (e.g., Thomson and Armstrong, 1987; Eldredge et al., 1993; Thomson et al., 1996; Irmak and Haman, 2001; Leib et al., 2003; Varble and Chávez, 2011; Rudnick et al., 2015; Singh et al., 2019; Chen et al., 2019). However, the elusive nature of universally accurate calibrations and of practical site-specific calibration methods is not the sole remaining technical challenge for the successful use of soil moisture sensors.

Soil moisture sensor data are known to be spatially variable (Hupet and Vanclooster, 2002; Wilson et al., 2004). Predictable patterns governed by soil forming factors (Lo et al., 2017), unpredictable deviations arising from microscale phenomena (e.g., preferential flow, root distribution; Logsdon, 2009), and disparities imposed intentionally or unintentionally by management (Coelho and Or, 1996) can all contribute to the spatial variability of true soil water status. Moreover, multiple units of the same soil moisture sensor can report unequal values given equal true soil water status because the physical and electrical properties of the sensor hardware (Kelleners et al., 2005) or the soil disturbance from sensor installation (Rothe et al., 1997) is not identical. If the variability in soil moisture sensor data is too large within a supposedly uniform field, the difficulty of precisely estimating mean true soil water status can be a major obsta-

Submitted for review in January 2020 as manuscript number NRES 13918; approved for publication as a Research Article part of the NIS Collection by the Natural Resources & Environmental Systems Community of ASABE in April 2020.

The authors are **Tsz Him Lo**, Assistant Professor of Irrigation Engineering, National Center for Alluvial Aquifer Research, Mississippi State University, Leland, Mississippi; **H. C. (Lyle) Pringle, III**, Associate Agricultural Engineer, Delta Research and Extension Center, Mississippi State University, Stoneville, Mississippi; **Daran R. Rudnick**, Assistant Professor and Irrigation Management Specialist, **Geng Bai**, Research Assistant Professor, Department of Biological Systems Engineering, University of Nebraska-Lincoln, Lincoln, Nebraska; **L. Jason Krutz**, Professor and Director, Mississippi Water Resources Research Institute, Mississippi State University, Starkville, Mississippi; **Drew M. Gholson**, Assistant Professor and Irrigation Specialist, National Center for Alluvial Aquifer Research, Mississippi State University, Leland, Mississippi; and **Xin Qiao**, Assistant Professor and Irrigation Management Specialist, Panhandle Research and Extension Center, University of Nebraska–Lincoln, Scottsbluff, Nebraska. **Corresponding author:** Tsz Him Lo, P. O. Box 197, Stoneville, MS 38776; phone: 662-686-9311; email: himmy.lo@msstate.edu.

  ISSN 0883-8542 https://doi.org/10.13031/aea.13918

cle to the successful use of soil moisture sensors. This problem can hinder researchers from discerning differences between treatments and can hinder practitioners from making informed decisions.

The magnitude of variability in soil moisture sensor data within macroscopically homogeneous environments has been found to vary jointly with the sensor model and with the surrounding environment (Schmitz and Sourell, 2000; Evett et al., 2009; Rosenbaum et al., 2010; Lo et al., 2020). The limitations in design and manufacturing can differ among sensor models, whereas the prominence of microscale phenomena can change with the surrounding environment. In turn, the interaction of both factors can dictate the susceptibility of a sensor model to the influence of microscale phenomena. Therefore, each model—or at least each type—of soil moisture sensor should be examined specifically to characterize its data variability in an appropriate range of field conditions.

Granular matrix sensors (GMS) can be used to estimate soil water tension by measuring the moisture-dependent electrical resistance of the encased porous material because this material is hydraulically connected to and thus exchanges moisture with the surrounding soil (Scanlon et al., 2002). Previous research has investigated the data variability among multiple units of the same GMS model in several macroscopically homogeneous environments—in a temperature-controlled pressure plate apparatus (McCann et al., 1992), in repacked soil tanks (Sui et al., 2019), in a repacked and grassed soil tank (Shock et al., 1998), under outdoor turf in a loamy sand (Schmitz and Sourell, 2000), and under greenhouse vegetables in a layered and medium textured soil (Thompson et al., 2006). However, in macroscopically homogeneous environments involving agronomic crop production, the data variability among multiple units of the same GMS model has not been commonly reported.

For agronomic crops, GMS are typically installed in sets, each of which consists of multiple sensors that are in close horizontal proximity but are distributed at different depths within the managed root zone profile. Producers are often recommended to schedule irrigation by delaying water application until the GMS set(s) reported a profile average soil water tension value that is drier than a predetermined threshold (Irmak et al., 2016; Henry et al., 2018). Yet, some studies such as Tollner et al. (1991) and Schmitz and Sourell (2000) have claimed based on probability theory that a large number of sensor sets is necessary for successful irrigation scheduling. Notwithstanding, irrigation scheduling with just one sensor set has been reported to reduce applied irrigation while maintaining or even improving crop yield relative to producer practice (Bryant et al., 2017; Spencer et al., 2019). Such results are partly attributed to the vast disparity between optimal management and the current practice of some producers. Nonetheless, the experimental evidence motivates a revisit of the pertinent probability theory.

The first objective of this article is to describe the variability in GMS data within two macroscopically homogeneous, fine textured soybean fields. The second and more important objective of this article is to delve into the implications of within-field variability in GMS data for irrigation scheduling. Specifically, traditional and alternate assumptions in the interpretation of this variability are elucidated and then are compared in terms of effect on the choice of sensor set number and irrigation triggering threshold for achieving a target level of irrigation adequacy.

Field Study

Data Collection

Research Sites

This article relied on GMS data from a field study at the Mississippi State University Delta Research and Extension Center. This field study was conducted in 2018 and 2019 on two contiguous rectangular fields (33.403°N, 90.935°W), each with a cropped area of 6 ha. Both fields were mapped as a Sharkey soil (Very-fine, smectitic, thermic Chromic Epiaquerts) by the Natural Resources Conservation Service soil survey (Soil Survey Staff, 2020). Analysis by the Mississippi State University Extension Service Soil Testing Laboratory (Starkville, Miss.) reported a textural composition of 2% sand, 47% silt, and 51% clay for the top 0.76 m of soil. Other soil physical properties have not been measured.

Both fields had been precision graded to a 0.1% slope back in 2009. Since then, the fields have been furrow irrigated and have received tillage by a disk harrow and/or by an integral disk bedder whenever deemed beneficial. In both years and on both fields, soybeans were planted at a rate of 346,000 seeds ha^{-1} in a twin row configuration following soybeans. The row spacing was 0.18 m within each pair of twin rows and 0.84 m between pairs. The planting dates were 18 May 2018 and 24 May 2019 on the eastern field (hereafter "A") and were 2 May 2018 and 30 April 2019 on the western field (hereafter "B").

Granular Matrix Sensors

Usually around three or four weeks after planting each year (with the exception of field B in 2019 because of delays by flooding), a set of Watermark Model 200SS (Irrometer Company, Riverside, Calif.) GMS was installed halfway between a pair of interior twin rows in each of 24 plots per field (fig. 1). Along the crop row direction, the distance from the higher end of a field to each of its 24 sensor set locations was ½- ⅔ of the 150-m total crop row length. The sensor set at each location consisted of three individual sensors—one at a depth of 0.20 m, one at a depth of 0.40 m, and one at a depth of 0.60 m—that were also 0.2 m apart from each other along the crop row direction. For installing each sensor after it had been glued to a section of polyvinyl chloride (PVC) pipe, an electrically powered auger was first used to create a vertical hole with the same diameter as the sensor-PVC assembly. A slurry of local soil was then poured into the hole, and the sensor-PVC assembly was finally inserted to place the center of the sensor at the desired depth. Several days after installation, all sensors were connected to a non-commercial wireless datalogger network (Fisher and Gould, 2012). The dataloggers converted sensor electrical resistance to soil water tension according to the Shock et al. (1998) calibration equation for the Watermark Model 200SS while assuming a constant sensor temperature of 25°C. At the start of each hour, the base station retrieved and recorded the instantaneous soil water tension

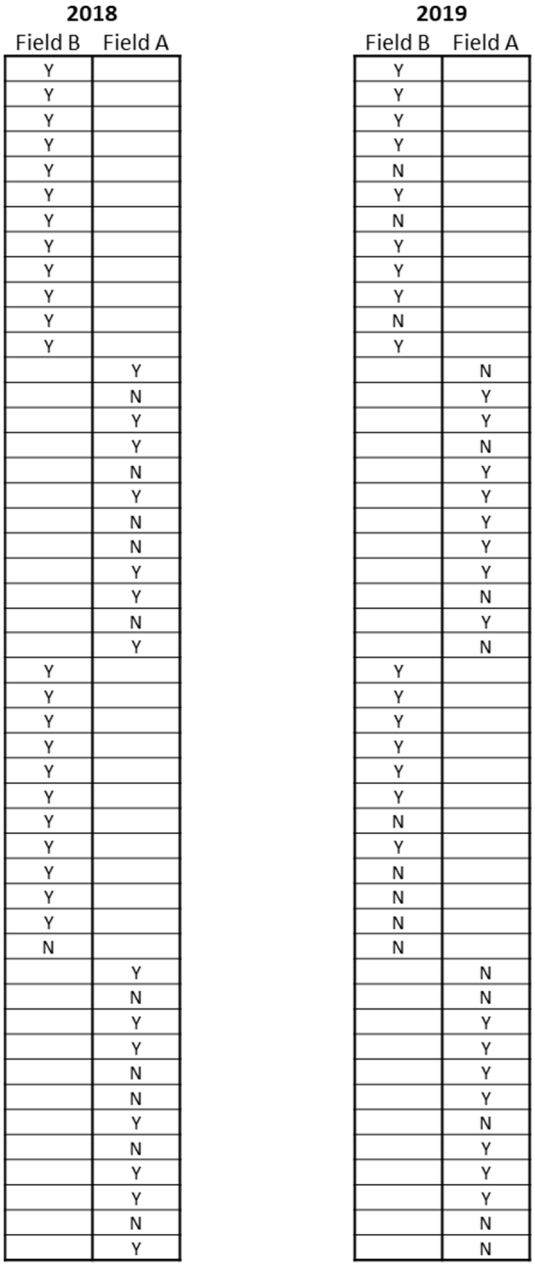

Figure 1. Diagram of sensor set locations in the field study; each rectangular cell represents an 8.1 m wide × 150 m long plot, and sensor sets that were included and excluded from analysis were indicated with "Y" and "N", respectively.

value from each sensor. Throughout this article, tension refers to the additive inverse of soil water pressure, so tension increases from low to high as a soil dries.

Only a subset of the original dataset in each site-year was appropriate for analyzing within-field variability in GMS data (table 1). This subset began at least a week after sensor installation to allow sensors to equilibrate with surrounding soil. This subset ended the day before the first irrigation of that site-year because the various sensor sets received different irrigation treatments in the field study. Carryover of irrigation treatment effects between years was not a concern because rainfall was abundant during the off-season and the early season. A sensor set was omitted entirely if its data were determined to be blatantly unrealistic or contained multi-day gaps owing to problems in the wireless datalogger network. To simplify comparisons amidst sub-day data gaps, the remainder of the article focused on the maximum tension value of each sensor on each calendar date, noting that the daily maximum is typically the most important value for irrigation scheduling. Throughout this article, the profile average tension of a sensor set was calculated as the unweighted arithmetic mean of the tension values reported by its three sensors (at 0.20, 0.40, and 0.60 m, respectively). All computations were performed in Excel 2010 (Microsoft Corporation, Redmond, Wash.).

Weather Conditions

Weather conditions during the analyzed part of each site-year are summarized in table 1. Daily rainfall was measured by a manual rain gauge at the northwest corner of field B. Daily short reference evapotranspiration (ET_o; Allen et al., 1998) was calculated by the Mississippi State University Delta Agricultural Weather Center (http://deltaweather.extension.msstate.edu) from its Stoneville manual weather station located 4 km northeast of the two fields. In both 2018 and 2019, the GMS data from field A could be divided into two distinct drying periods. The rain events on 19 and 21 June separated the two periods in 2018, whereas the rain events on 14-16 July separated the two periods in 2019. In both years, the GMS data from field B consisted of essentially one drying period.

DATA DESCRIPTION

Temporal Trends

The temporal trends in the GMS data matched the expectations that tension should decrease with rainfall and increase with crop water use (fig. 2-3). Light rains decelerated the rate of tension increase, whereas heavy rains decreased tension sharply. More frequently at shallower depths, tension at all locations would fall within a narrow tension range between 8 and 12 kPa in response to a heavy rain, resulting in very low within-field variability. As drying resumed, the tension differences among locations began to expand. The daily rate of tension increase at some locations deviated drastically from the field average daily rate, sometimes even by a factor of two (faster or slower), which caused within-field variability to widen.

Temporal Stability

To examine the temporal stability of the within-field variability in GMS data, Spearman's rank correlation coefficient was calculated between the location rankings by depth-specific tension on each date and the location rankings by depth-specific tension on the date with the highest profile average tension. This driest date was the final date of the dataset in all site-years except field A in 2019, when it occurred on 14 July at the end of the first drying period. If tension tended to be higher at some particular locations and lower at some other particular locations, then the rankings on most dates would be similar to the rankings on the driest date, which would result in rank correlation coefficient values approaching 1.

Table 1. The subset of granular matrix data from each site-year that was used in this article.

Site-Year	Field A in 2018	Field A in 2019	Field B in 2018	Field B in 2019
First day	16 June	22 June	5 June	21 June
Last day	3 July	25 July	12 June	9 July
Total sensor sets	14	15	23	16
Average ET_o (mm d^{-1})	5.2	5.1	5.5	5.1
Dates with rainfall > 2.5 mm	19 June (16 mm) 21 June (18 mm) 29 June (6 mm)	24 June (119 mm) 29 June (4 mm) 4 July (5 mm) 7 July (7 mm) 14-16 July (114 mm)	None	24 June (119 mm) 29 June (4 mm) 4 July (5 mm) 7 July (7 mm)

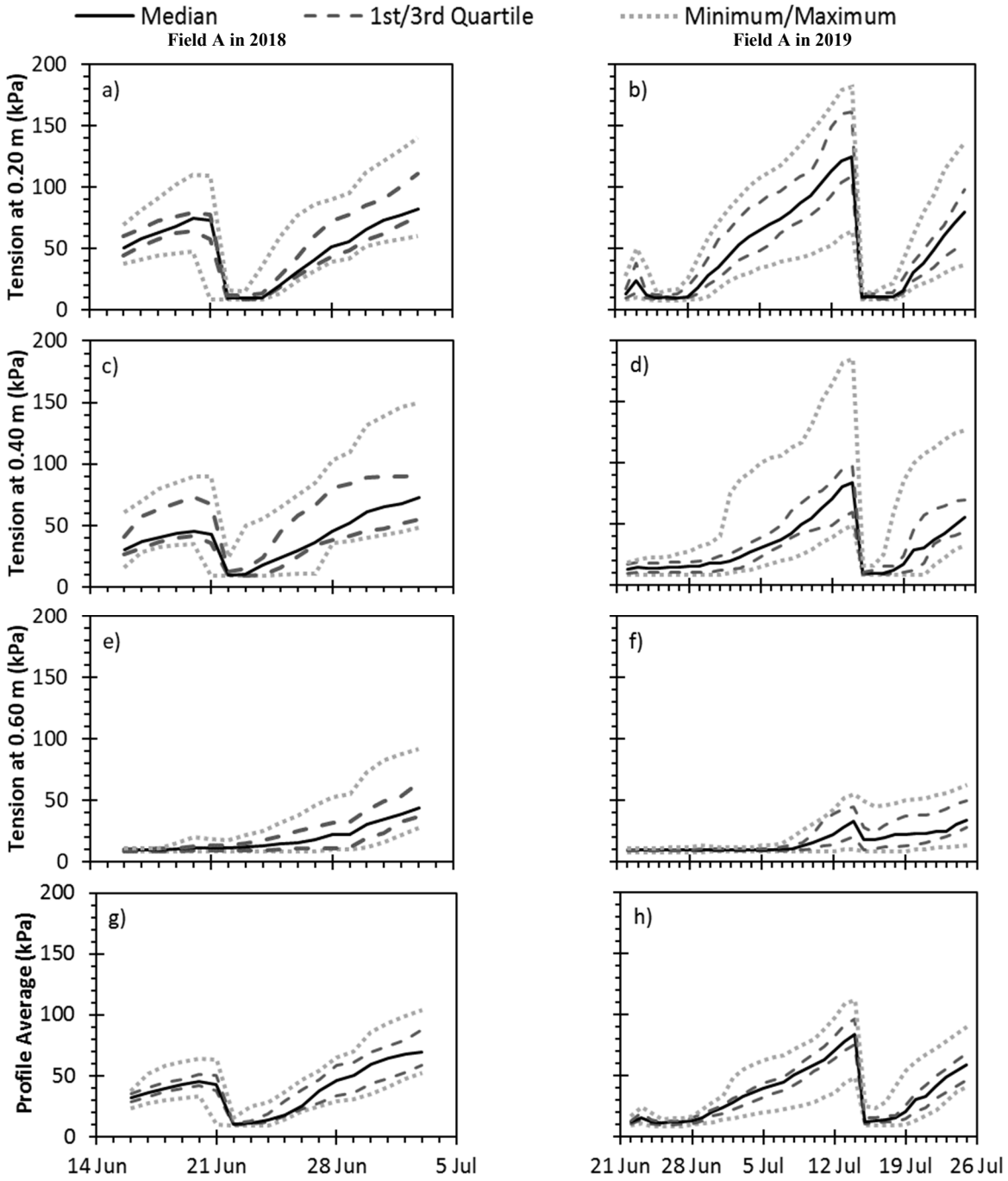

Figure 2. Soil water tension at the three sensor depths individually (subfigures a-f) and averaged (subfigures g-h) within field A among 14 locations in 2018 and among 15 locations in 2019; lower tension values are wetter, and higher tension values are drier.

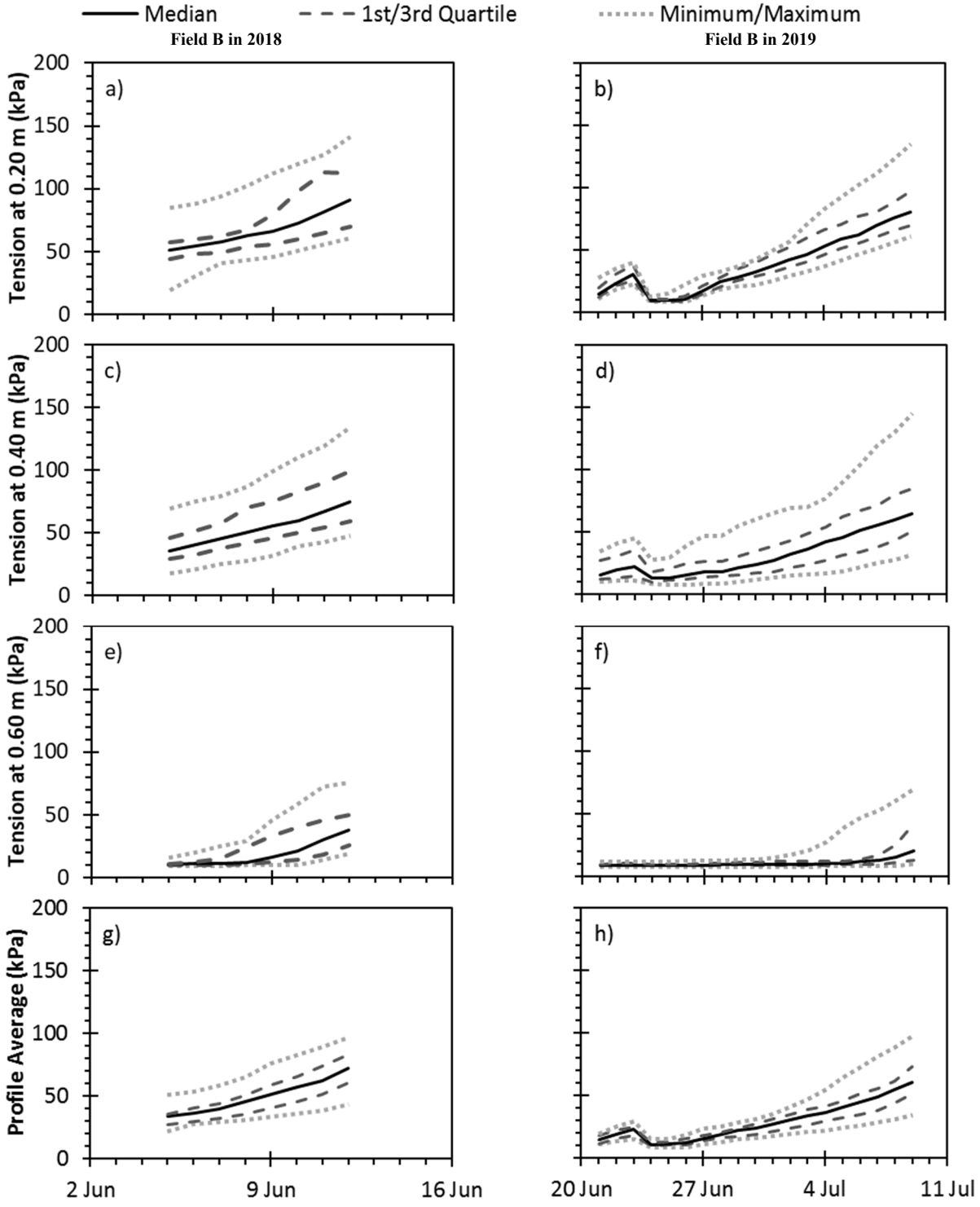

Figure 3. Soil water tension at the three sensor depths individually (subfigures a-f) and averaged (subfigures g-h) within field B among 23 locations in 2018 and among 16 locations in 2019; lower tension values are wetter, and higher tension values are drier.

Except within several days after a heavy rain, Spearman's rank correlation coefficient was generally above 0.5 for all depths (fig. 4). The coefficient was especially high within a few days before the driest date but was increasing over time even during drying periods that did not culminate in the driest date. The depth exhibiting the highest temporal stability was inconsistent among the four site-years. Overall, the results suggest that deviations from the field mean by sensor locations were moderately systematic within a site-year. Further research could explore whether the tendency for above/below average tension at a sensor location carries over between years (Van Pelt and Wierenga, 2001).

Probability Distribution

Fitting the within-field variability in GMS data to a known type of probability distribution would benefit the description of this variability. As the variability on the driest

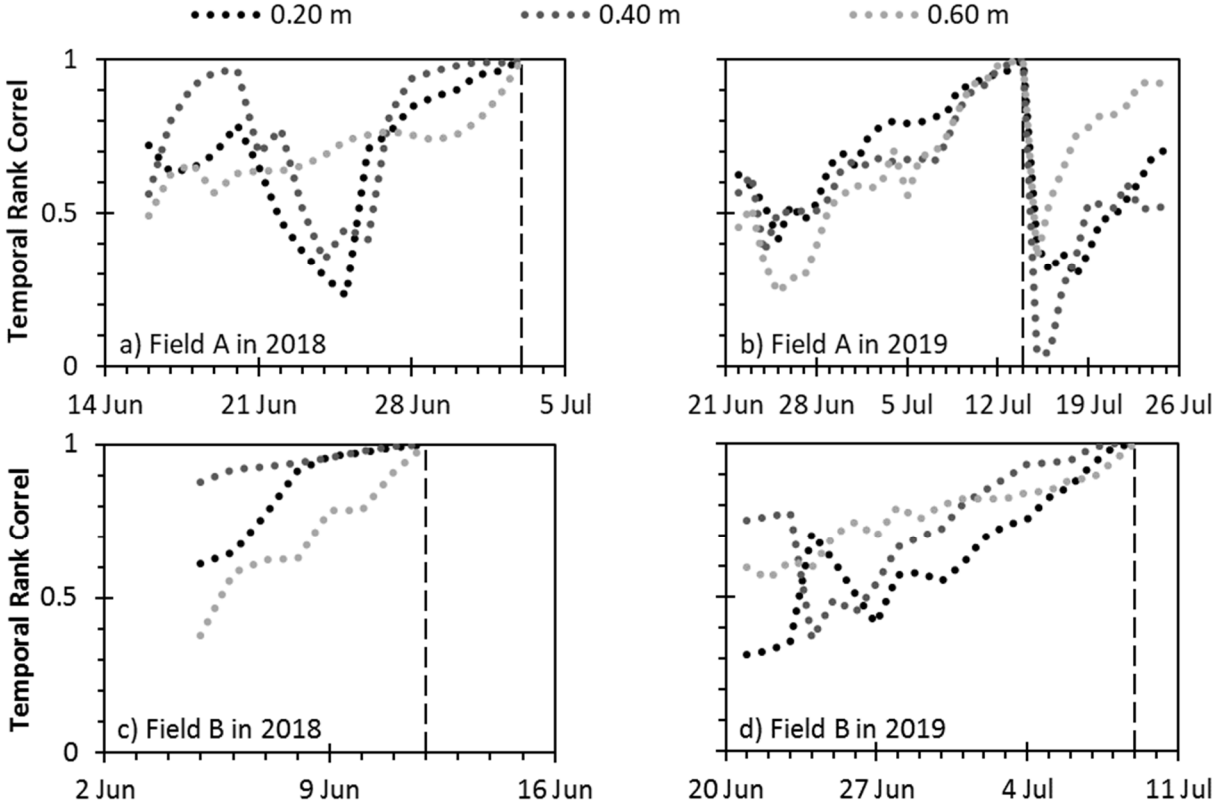

Figure 4. Spearman's rank correlation coefficient between the location rankings by soil water tension on each measurement date and the location rankings by soil water tension on the driest date (marked by the vertical dashed line) in a site-year; the coefficient approaches 1 as the two sets of rankings become more similar.

date is expected to be most similar to the variability on an actual irrigation decision date, a quantile-quantile plot was constructed to evaluate the normality of the GMS data on the driest date of each site-year (fig. 5). For field A in 2018 and 2019, the fit was generally satisfactory ($R^2 > 0.95$), with the largest discrepancies occurring at intermediate values of cumulative probability (i.e., near the field mean). For field B in 2018 and 2019, the fit was quite good ($R^2 > 0.98$). Overall, within-field variability in GMS data appeared to be approximately normal. Approximate normality of tension data was reported by Schmitz and Sourell (2000) on most measurement dates and by Van Pelt and Wierenga (2001) on some measurement dates.

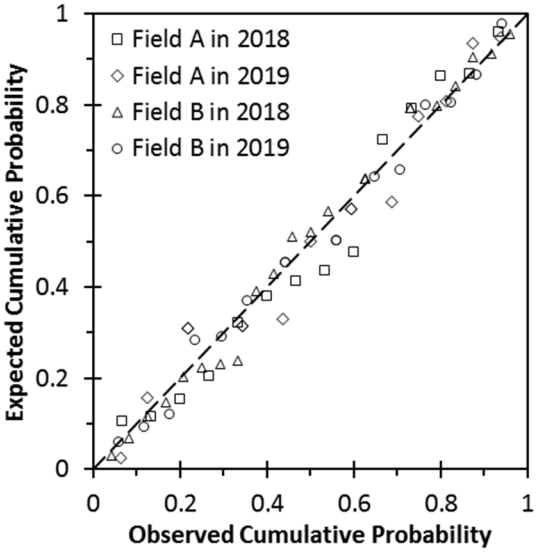

Figure 5. Scatterplot of expected cumulative distribution (assuming normality) vs. observed cumulative distribution (according to Weibull plotting position) for profile average soil water tension among sensor set locations on the driest date in each site-year; datasets that follow closely the dashed 1:1 line appear to be normally distributed.

Mean-Variance Relationship

A normal distribution can be specified using just two parameters—its mean and its variance. If a relationship was found between the mean and the variance of GMS data, then the normal distribution of GMS data could be predicted from the mean alone. Indeed, sample variance in tension increased with increasing sample mean tension for every depth and for the profile average in every site-year (fig. 6). This observation agrees with figures 2-3, where the spread in tension data widened as drying progressed. Positive association between mean and variance in tension was also reported by Schmitz and Sourell (2000), Van Pelt and Wierenga (2001), and Thompson et al. (2006). In the present field study, the relationship was generally linear, but the exact slope and intercept differed among depths and among site-years. The magnitude of the regression slope in figure 6d is about ⅓-½ the magnitude of the regression slopes in figures 6a-c, so the within-field variability in profile average tension was clearly smaller than the within-field variability in tension at individual depths.

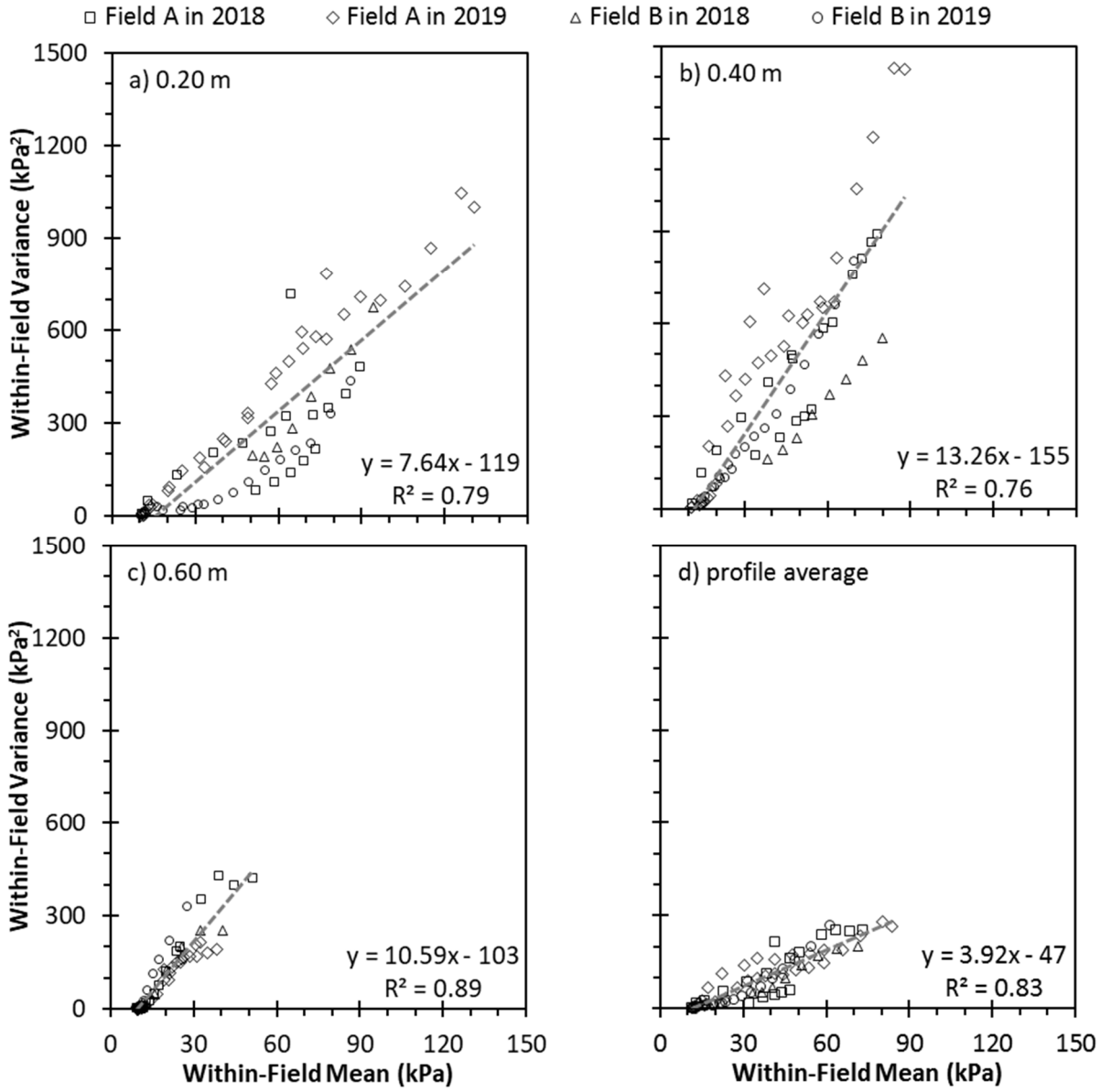

Figure 6. Within-field variance versus within-field mean of soil water tension for the three sensor depths individually (subfigures a-c) and for the profile average (subfigure d).

To obtain a preliminary idea of whether the regression equations that were fitted to pooled data across site-years were valid, literature values of standard deviation in tension were used for comparison. At a mean tension of 30-40 kPa at a depth of 0.30 m, Hendrickx et al. (1994) reported standard deviation values of 4.3-12.3 kPa among 15-34 locations. The regression equations in figure 6a and 6b for depths of 0.20 and 0.40 m predict standard deviation values of 12.2 and 17.6 kPa given a mean of 35 kPa. At a mean profile average tension of 45-55 kPa across three depths, Van Pelt and Wierenga (2001) reported standard deviation values of 10.1-12.9 among 52-57 locations. The regression equation in figure 6d for the profile average across three depths predicts a standard deviation of 12.2 kPa given a mean of 50 kPa. Although such checks could not be performed at higher mean tension because the pertinent previous studies were conducted using tensiometers, the regression equations seem to provide reasonable estimates of variance in tension for macroscopically homogeneous fields.

Implications for Irrigation Scheduling

Conceptual Framework

Relevant and Irrelevant Variability

The implications of within-field variability in soil moisture sensor data for irrigation scheduling hinge on the interpretation of this variability. Evett et al. (2009) explained and demonstrated how this variability consists of 1) variability that is relevant to the purpose of measurement and 2) variability that is irrelevant to this purpose. This concept is highlighted in equation 1. For the purpose of irrigation scheduling, relevant variability refers to variability at the spatial scale where nonuniformity in soil water status affects

crop yield. Relevant variability is a property of the environment being measured and is thus independent of the sensor model being used. Lumping together all remaining variability—regardless of attribution to phenomena at finer spatial scales, to intrinsic issues of a sensor model, and/or to any interactions between the two factors—irrelevant variability is dependent on both the environment being measured and the sensor model being used.

$$\textit{Within-Field Variability in Sensor Data} = \textit{Relevant Variability} + \textit{Irrelevant Variability} \quad (1)$$

Simplifications

Regrettably, it is infeasible in practice to partition sensor data variability into relevant and irrelevant variability for each sensor model in each environment through thorough experimentation. Without prior knowledge, a user might adopt one of two simplifying assumptions. The traditional view on sensor data variability is exemplified by the discussion in Schmitz and Sourell (2000). It assumes relevant variability to be negligible and treats all sensor data variability as irrelevant variability. Thus, this view concludes that there is one relevant profile average tension value (or volumetric water content) in a field at a given time, which can be more precisely estimated by using a larger number of sensor sets. An alternate view is completely the opposite. It assumes irrelevant variability to be negligible and treats all sensor data variability as relevant variability. Thus, this view concludes that relevant profile average tension (or volumetric water content) is a spatial distribution (rather than a single value), which itself is uninfluenced by sensor set number but whose mean can be more precisely estimated by using a larger number of sensor sets.

General Case

The chosen interpretation, in turn, dictates how sensor set number and irrigation triggering threshold are thought to affect irrigation adequacy when scheduling irrigation. The general case, described by equation 2 and figure 7a, covers the full range of possibilities spanned by the traditional view on one extreme and the alternate view on the opposite extreme. Readers should note that this article adheres to the convention that uppercase symbols represent random variables whereas lowercase symbols represent specific values. In the conceptual framework of this article, the magnitude by which the irrigation triggering threshold x_n is lower than the critical water stress threshold c acts as insurance against within-field variability in sensor data and serves as the crop water supply during multi-day irrigation cycles.

$$A = F\left(c \mid F^{-1}\left(P \mid x_n, \frac{\sigma^2_{sensor}}{n}\right), \sigma^2_{relevant}\right) \quad (2)$$

where

A = expected probability distribution of the area fraction (unitless) with adequate soil water under the irrigation system,

$F(x|y,z)$ = function returning the cumulative probability (unitless) of a random variable being less than the value x if this variable follows a normal distribution with mean y and variance z,

c = critical water stress threshold (kPa),

$F^{-1}(p|y,z)$ = function returning the value (same units as y) corresponding to a cumulative probability p for a normal distribution with mean y and variance z,

P = a random variable (unitless) that follows a uniform distribution bounded between 0 and 1,

n = total number (unitless) of sensor sets,

x_n = sample mean profile average tension (kPa) among n sensor sets, at which irrigation is triggered,

σ^2_{sensor} = within-field variance in profile average tension (kPa^2) as reported by sensor data,

$\sigma^2_{relevant}$ = within-field variance in profile average tension (kPa^2) at the relevant spatial scale (i.e., the scale at which tension nonuniformity affects crop yield).

Traditional And Alternate Views

With the traditional view, the assumption of $\sigma^2_{relevant} = 0$ transforms equation 2 and figure 7a into equation 3 and figure 7b, respectively. Mathematically, A in equation 2 becomes a discrete distribution where the probability of $A = 1$ equals a in equation 3 and where the probability of $A = 0$ equals $1 - a$. The expected value of A is then equal to a in

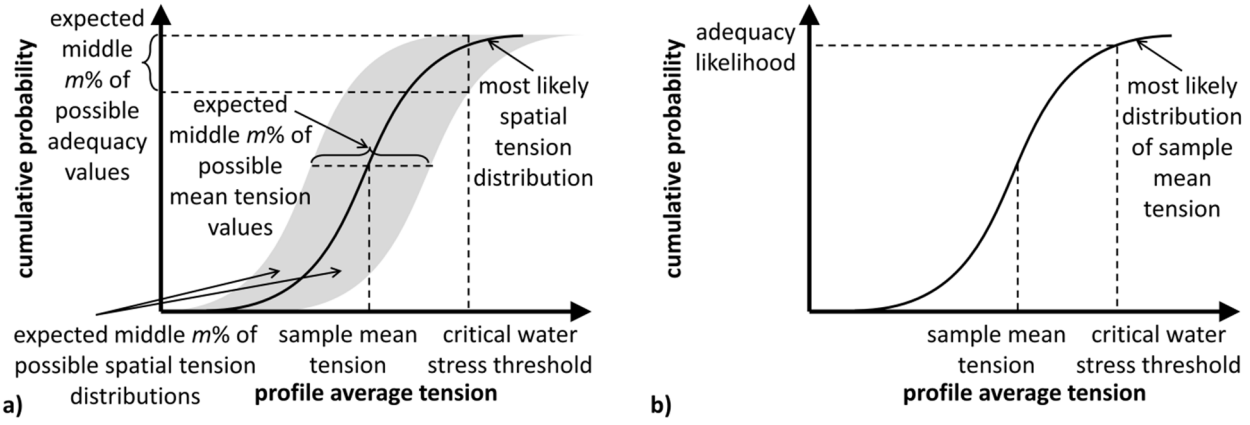

Figure 7. Conceptual diagrams for a) the general case and b) the traditional view of within-field variability in soil water tension data; subfigure a also describes the alternate view.

equation 3. Conceptually, the traditional view allows only two possible scenarios at a given point in time. In the absence of relevant variability, the land under an irrigation system is either entirely adequate in soil water (i.e., all below the critical water stress threshold c) or entirely inadequate in soil water (i.e., all above the critical water stress threshold c). Therefore, a in equation 3 represents the likelihood of adequacy and is increased by increasing sensor set number if $x_n < c$ and by lowering the irrigation triggering threshold x_n.

$$a = F\left(c \mid x_n, \frac{\sigma^2_{sensor}}{n} \right) \tag{3}$$

where a = likelihood (unitless) of the adequate area fraction equaling 1 under the irrigation system

The alternate view shares figure 7a with the general case. Substituting the assumption of $\sigma^2_{relevant} = \sigma^2_{sensor}$ into equation 2, equation 4 is obtained for the alternate case. Lowering the irrigation triggering threshold shifts the curve and the grey band all to the left, which shifts the distribution A higher. Increasing sensor set number reduces uncertainty in mean relevant tension and thus shrinks the width of the grey band and the spread in A. However, the shape of the curve and of the grey band is controlled by relevant variability and cannot be modified by sensor set number.

$$A = F\left(c \mid F^{-1}\left(P \mid x_n, \frac{\sigma^2_{sensor}}{n} \right), \sigma^2_{sensor} \right) \tag{4}$$

Additional Assumptions

The present analysis assumed that within-field variability in tension sensor data follows normal distributions. As reviewed in the previous section, approximate normality in tension sensor data is commonly reported in the literature. This assumption also removes the need to check for normality using the small number of sensors that are prevalent in practice. The overall conceptual framework is compatible with any type of probability distribution, but the specific equations would obviously need to be modified if within-field variability in tension sensor data followed non-normal distributions.

The present analysis also assumed that the relevant within-field variance in tension sensor data can be predicted, which is like power analysis in experimental design. This assumption is especially convenient because it avoids the problem of estimating variances using a small number of sensors and also allows the use of the normal (i.e., z) distribution rather than the Student's t distribution. Preliminary results in the previous section suggest that predicting variances might be feasible. Nevertheless, further research on the within-field variance in tension sensor data—with different combinations of sensor models and environments—would be required to support fully the operational prediction of these variances.

APPLICATION

Procedures

Equations 3 and 4 were applied to assess the quantitative impact of sensor set number and irrigation triggering threshold on irrigation adequacy when scheduling irrigation using GMS. The value a in equation 3 was computed directly, while the distribution A in equation 4 was computed using a 10000-point approximation for the distribution P. The value of σ^2_{sensor} was estimated using the regression equation in figure 6d, which is reproduced below as equation 5. For σ^2_{sensor} in equation 3 and for the first instance of σ^2_{sensor} in equation 4, the sample mean tension x_n was plugged into equation 5. Yet for the second instance of σ^2_{sensor} in equation 4, each result of the inverse cumulative distribution function F^{-1}—representing a possible relevant mean tension value—was plugged into equation 5. Extrapolating equation 5 beyond the range of tension from which it was developed (<84 kPa) could be risky. However, figure 6a, which witnessed a wider range of tension (<131 kPa), suggests that the linear relationship between mean and variance should continue at higher tension values. The critical water stress threshold was assumed to be 100 kPa loosely based on Bryant et al. (2017).

$$\sigma^2_{sensor} = 3.92x - 47 \tag{5}$$

where x = mean profile average tension (kPa)

Traditional View of Variability

Figure 8a illustrates the impact of sensor set number and irrigation triggering threshold on irrigation adequacy assuming single-day irrigation cycles and the traditional view of GMS data variability. Adequacy likelihood increases at a decreasing rate as the irrigation triggering threshold decreases away from the critical water stress threshold. Adequacy likelihood increases most with increasing sensor set number when sensor set number equals 1 and irrigation triggering threshold is moderately below the critical water stress threshold. The curves in figure 8a are slightly asymmetrical because the variance was modeled to increase with the mean (eq. 5).

Alternate View of Variability

Figures 9a-c illustrate the impact of sensor set number and irrigation triggering threshold on irrigation adequacy assuming single-day irrigation cycles and the alternate view of GMS data variability. Expected mean adequacy increases at a decreasing rate as the irrigation triggering threshold decreases away from the critical water stress threshold. The expected adequacy distribution is widest when sensor set number equals 1 and irrigation triggering threshold is near the critical water stress threshold. Sensor set number exerts a slight increasing effect on expected mean adequacy when the irrigation triggering threshold is moderately below the critical water stress threshold. This effect is attributed to the strong left skew of the expected adequacy distribution within this range of irrigation triggering thresholds. As sensor set number increases, expected mean adequacy is consequently influenced more dramatically by the reduction in the long tail of low adequacy values than by the reduction in the short tail of high adequacy values. Expected mean adequacy is up to 0.07 higher for 10 sensor sets than for 1 sensor set within this range of irrigation triggering thresholds.

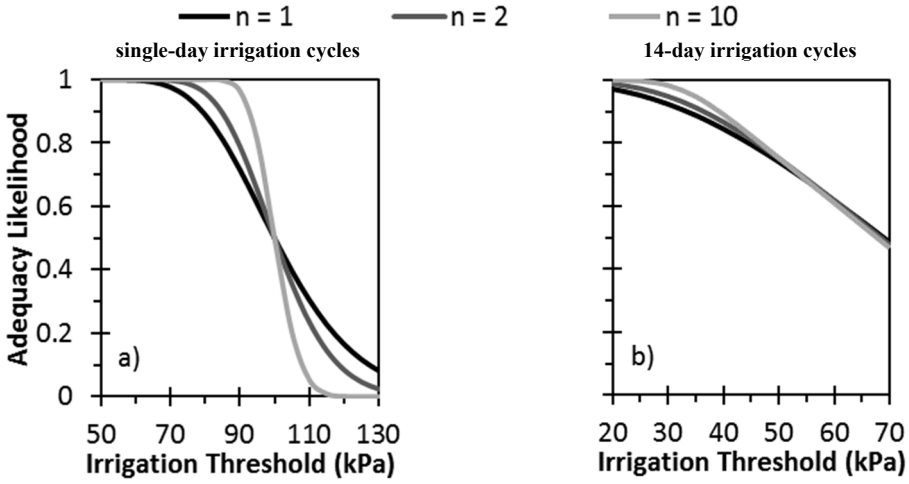

Figure 8. Adequacy likelihood for different numbers of sensor sets (*n*) assuming a critical water stress threshold of 100 kPa and the traditional view of within-field variability in granular matrix sensor data.

Single-Day Comparisons

The two opposing views of within-field variability in GMS data could be compared in terms of how sensor set number (*n*) changes the irrigation triggering threshold for achieving a target value of irrigation adequacy. A higher irrigation triggering threshold for the same irrigation adequacy is desirable because irrigation costs and overirrigation risks are reduced when depleting more stored soil water and leaving more capacity for holding future rainfall. Assuming the traditional view, increasing sensor set number from 1 to 10 increases the irrigation triggering threshold from 86 to 95 kPa for an adequacy likelihood of 0.80, from 79 to 93 kPa for an adequacy likelihood of 0.90,

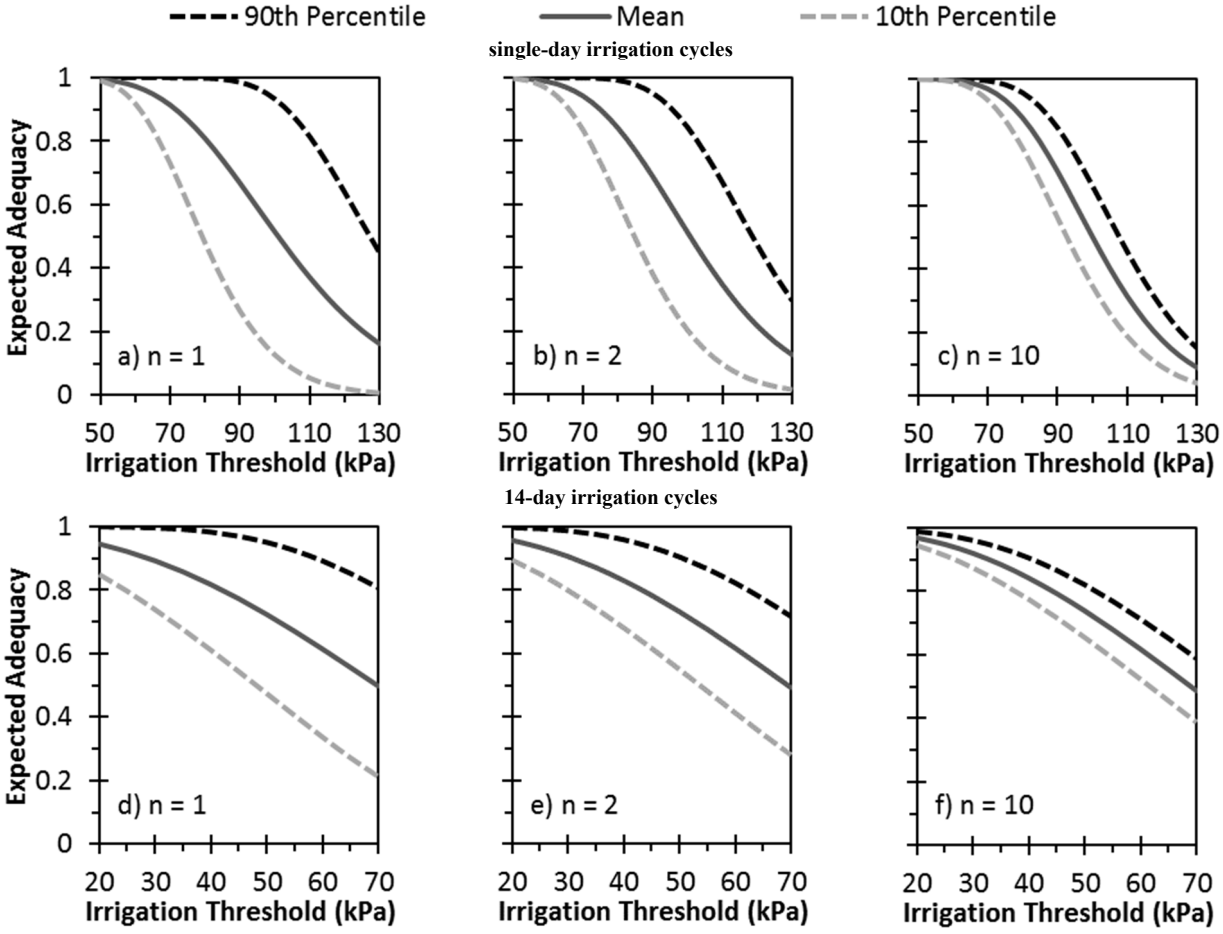

Figure 9. Expected mean and middle 80% of irrigation adequacy for different numbers of sensor sets (*n*) assuming a critical water stress threshold of 100 kPa and the alternate view of within-field variability in granular matrix sensor data.

and from 66 to 87 kPa for an adequacy likelihood of 0.99 (fig. 8a). Assuming the alternate view, increasing sensor set number from 1 to 10 increases the irrigation triggering threshold from 81 to 85 kPa for an expected mean adequacy of 0.80, from 72 to 78 kPa for an expected mean adequacy of 0.90, and from 54 to 64 kPa for an expected mean adequacy of 0.99 (figs. 9a and 9c). The increases in irrigation triggering threshold from increasing sensor set number are roughly twice as large assuming the traditional view than assuming the alternate view. This finding may seem counterintuitive initially but can be explained as follows. According to the traditional view that there is only one relevant tension value, a large sensor set number provides a precise estimate of this particular value and enables near-perfect irrigation scheduling. Yet according to the alternate view that there is a spatial distribution of relevant tension values, increasing sensor set number provides a more precise estimate of the mean but never eliminates the presence of high relevant tension values that always drag down expected mean adequacy.

Multi-Day Comparisons

In production settings, multi-day irrigation cycles are common. The graphs representing single-day irrigation cycles (figs. 8a and 9a-c) can be used to develop graphs representing multi-day irrigation cycles. Given an irrigation triggering threshold at the start of the multi-day cycle and an expected daily rate of tension increase over the *k* days of the cycle, a series of *k* relevant tension values (traditional view) or mean relevant tension values (alternate view) can be generated, each of which is the effective irrigation triggering threshold on its corresponding day. By superimposing the single-day adequacy likelihood (traditional view) or expected adequacy distribution (alternate view) for each of the *k* irrigation triggering thresholds, the cycle-wide likelihood or distribution can be calculated. Here, the length of the irrigation cycle was assumed to be 14 days, and the expected daily rate of tension increase was assumed to be 5 kPa d^{-1} loosely based on the field study. If the irrigation triggering threshold at the start of the cycle was 20 kPa, for example, the 14 associated daily irrigation thresholds were 20, 25, 30, 35, 40, 45, 50, 55, 60, 65, 70, 75, 80, and 85 kPa.

Figures 8b (traditional view) and 9d-f (alternate view) illustrate the impact of sensor set number and irrigation triggering threshold on irrigation adequacy assuming 14-day irrigation cycles. Assuming the traditional view, increasing sensor set number from 1 to 10 increases the irrigation triggering threshold from 45 to 47 kPa for an adequacy likelihood of 0.80 and from 33 to 39 kPa for an adequacy likelihood of 0.90. Assuming the alternate view, increasing sensor set number from 1 to 10 increases the irrigation triggering threshold from 42 to 44 kPa for an expected mean adequacy of 0.80 and from 28 to 32 kPa for an expected mean adequacy of 0.90. The increases in irrigation triggering threshold from increasing sensor set number are smaller for 14-day cycles than for single-day cycles, especially if assuming the traditional view. Because a long cycle is typically paired with a low irrigation triggering threshold, a substantial portion of a long cycle is associated with relatively low variability (eq. 5) and relatively high adequacy likelihood (traditional view) or expected mean adequacy (alternate view) regardless of sensor set number. By including such days when the impact of sensor set number on adequacy is minimal, the cycle-wide adequacy likelihood or expected mean adequacy becomes relatively insensitive to sensor set number. Interestingly, the differences in irrigation triggering threshold between the traditional and alternate views are also smaller for 14-day cycles than for single-day cycles.

Expected 10th Percentile Adequacy

Thus far, target irrigation adequacy had been specified in terms of expected mean adequacy when assuming the alternate view. Because some users may be most concerned about the potential for low adequacy when scheduling irrigation, specifying target adequacy in terms of expected 10th percentile adequacy was also explored. For single-day cycles, increasing sensor set number from 1 to 10 increases the irrigation triggering threshold from 75 to 88 kPa for an expected 10th percentile adequacy of 0.60 and from 61 to 73 kPa for an expected 10th percentile adequacy of 0.80 (figs. 9a and 9c). For 14-day cycles, increasing sensor set number from 1 to 10 increases the irrigation triggering threshold from 41 to 54 kPa for an expected 10th percentile adequacy of 0.60 and from 25 to 38 kPa for an expected 10th percentile adequacy of 0.80 (figs. 9d and 9f). Here, the increases in irrigation triggering threshold from increasing sensor set number were similar between single-day cycles and 14-day cycles. Additionally, these increases based on expected 10th percentile adequacy are distinctly larger than the increases based on expected mean adequacy. Increasing sensor set number reduces the spread of the expected adequacy distribution regardless of irrigation cycle length, which explains the consistent benefit of larger sensor set numbers to irrigation scheduling based on expected 10th percentile adequacy.

Final Thoughts on the Two Views

The article has not championed either the traditional view or the alternate view of within-field variability in GMS data. Instead, it has faithfully clarified both views and the respective implications on irrigation scheduling. Proving the irrelevance of all sensor data variability is just as difficult as proving the relevance of all sensor data variability. Data variability among GMS has been reported to be similar to data variability among tensiometers (Thompson et al., 2006), and doubling the surface area of regular tensiometer cups decreased the standard deviation in single-depth tension by less than 0.5 kPa on average (Hendrickx et al., 1994). The scarce evidence suggests that at least some of the GMS data variability within macroscopically homogeneous fields might be relevant for irrigation scheduling, so the reality is most likely partway between the two extreme views.

CONCLUSION

This article reported a few key findings regarding the implications of within-field variability in GMS data for irrigation scheduling. If all sensor data variability is assumed

to be irrelevant for irrigation scheduling, the benefit of additional sensor sets decreases dramatically as irrigation cycles lengthen (see sub-subsection "Multi-Day Comparisons"). For shorter irrigation cycles and adequacy targets based on averages, the benefit of additional sensor sets is smaller if all sensor data variability is assumed to be relevant rather than irrelevant for irrigation scheduling (see sub-subsection "Single-Day Comparisons"). If all sensor data variability is assumed to be relevant for irrigation scheduling, the benefit of additional sensor sets does not decrease with lengthening irrigation cycles when adequacy targets are based on possible lows rather than averages (see sub-subsection "Expected 10th Percentile Adequacy").

While a large number of sensor sets is certainly helpful to provide redundancy and enhance precision, just one sensor set per irrigation system can still be an extremely worthwhile initial step for irrigation scheduling in many contexts. A significant portion of irrigated agronomic crops are grown in medium to fine textured soils (i.e., lower water stress sensitivity per unit of tension) and under irrigation systems with multi-day cycles. Assuming multiple measurement depths and partial relevance of sensor data variability, the irrigation triggering threshold to achieve an expected mean adequacy target might be just slightly lower for one sensor set than for a large number of sensor sets. Therefore, on-farm investments in the purchase, installation, and maintenance of numerous sensor sets might be difficult to justify for resource conservation alone in the absence of substantial financial and/or legal penalties for overirrigation. Because many producers do not yet use any irrigation scheduling tool, promoting the adoption of the first set of soil moisture sensors per irrigation system may be a higher priority than promoting the adoption of additional sensor sets.

There is an important caveat though. In this article, data from all suspicious sensor sets in the field study were carefully eliminated. In practice, such quality control requires the user and/or service provider to possess sufficient expertise and to pay sufficient attention. Problems can generally be caught long before the irrigation season if installations are permanent or occur shortly after crop emergence. Without timely assessment and corrective action (e.g., repair, replacement, relocation), the resulting data will be misleading rather than beneficial for irrigation scheduling.

Extra considerations would be needed to construct a comprehensive decision support tool to inform the selection of an appropriate sensor set number and an appropriate irrigation triggering threshold for a specific situation. First, the within-field variability of soil moisture sensor data should be evaluated for more sensor models in more environments (Lo et al., 2020). Second, how the method and nonuniformity of irrigation applications alter this variability (Saddiq et al., 1985; Clemmens, 1991) should be better understood. Third, any significant temporal changes in the critical water stress threshold as a result of weather and/or growth stage (Sadras and Milroy, 1996; Thompson et al., 2007; Pringle et al., 2019) should be modeled. Fourth, a profit response curve that includes irrigation costs and both underirrigation and overirrigation yield losses should be incorporated. All colleagues are invited to build on the probabilistic conceptual framework in this article to advance practical irrigation scheduling.

Acknowledgements

This publication is a contribution of the National Center for Alluvial Aquifer Research and the Mississippi Agricultural and Forestry Experiment Station. This material is based upon work that is jointly supported by the Mississippi Soybean Promotion Board under project numbers 40-2018 and 40-2019 and by the Agricultural Research Service, United States Department of Agriculture, under Cooperative Agreement number 58-6001-7-001. The authors are grateful for weather data from the Mississippi State University Delta Agricultural Weather Center. The authors thank John Johnson for assisting the field study.

References

Allen, R. G., Pereira, L. S., Raes, D., & Smith, M. (1998). Crop evapotranspiration: Guidelines for computing crop water requirements. FAO Irrigation and Drainage Paper No. 56. Rome, Italy: United Nations FAO.

Bryant, C. J., Krutz, L. J., Falconer, L., Irby, J. T., Henry, C. G., Pringle III, H. C.,... Wood, C. W. (2017). Irrigation water management practices that reduce water requirements for Mid-South furrow-irrigated soybean. *Crop Forage Turfgrass Manag., 3*(1). https://doi.org/10.2134/cftm2017.04.0025

Chen, Y., Marek, G. W., Marek, T. H., Heflin, K. R., Porter, D. O., Moorhead, J. E., & Brauer, D. K. (2019). Soil water sensor performance and corrections with multiple installation orientations and depths under three agricultural irrigation treatments. *Sensors, 19*(13), 2872. https://doi.org/10.3390/s19132872

Clemmens, A. J. (1991). Irrigation uniformity relationships for irrigation system management. *J. Irrig. Drain. Eng., 117*(5), 682-699. https://doi.org/10.1061/(ASCE)0733-9437(1991)117:5(682)

Coelho, E. F., & Or, D. (1996). Flow and uptake patterns affecting soil water sensor placement for drip irrigation management. *Trans. ASAE, 39*(6), 2007-2016. https://doi.org/10.13031/2013.27703

Eldredge, E. P., Shock, C. C., & Stieber, T. D. (1993). Calibration of granular matrix sensors for irrigation management. *Agron. J., 85*(6), 1228-1232. https://doi.org/10.2134/agronj1993.00021962008500060025x

Evett, S. R., Schwartz, R. C., Tolk, J. A., & Howell, T. A. (2009). Soil profile water content determination: Spatiotemporal variability of electromagnetic and neutron probe sensors in access tubes. *Vadose Zone J., 8*(4), 926-941. https://doi.org/10.2136/vzj2008.0146

Fisher, D. K., & Gould, P. J. (2012). Open-source hardware is a low-cost alternative for scientific instrumentation and research. Modern Instrumentation. https://doi.org/10.4236/mi.2012.12002

Hendrickx, J. M. H., Nieber, J. L., & Siccama, P. D. (1994). Effect of tensiometer cup size on field soil water tension variability. *SSSAJ, 58*(2), 309-315. https://doi.org/10.2136/sssaj1994.03615995005800020007x

Henry, C. G., Francis, P. B., Espinoza, L., Ismanov, M., & Pickelmann, D. M. (2018). How to use Watermark soil moisture sensors for irrigation. Little Rock: Arkansas Cooperative Ext. Service. Retrieved from https://www.uaex.edu/environment-nature/water/How%20to%20use%20Watermark%20Factsheet%20July%202018.pdf

Hupet, F., & Vanclooster, M. (2002). Intraseasonal dynamics of soil moisture variability within a small agricultural maize cropped field. *J. Hydrol., 261*(1), 86-101. https://doi.org/10.1016/S0022-1694(02)00016-1

Irmak, S., & Haman, D. Z. (2001). Performance of the Watermark granular matrix sensor in sandy soils. *Appl. Eng. Agric., 17*(6), 787. https://doi.org/10.13031/2013.6848

Irmak, S., Payero, J. O., VanDeWalle, B. S., Rees, J. M., Zoubek, G. L., Martin, D. L.,... Leininger, D. (2016). Principles and operational characteristics of Watermark granular matrix sensors to measure soil water status and its practical applications for irrigation management in various soil textures. Ext. Circular EC783. University of Nebraska-Lincoln Ext. Retrieved from http://extensionpublications.unl.edu/assets/pdf/ec783.pdf

Kelleners, T. J., Seyfried, M. S., Blonquist Jr., J. M., Bilskie, J., & Chandler, D. G. (2005). Improved interpretation of water content reflectometer measurements in soils. *SSSAJ, 69*(6), 1684-1690. https://doi.org/10.2136/sssaj2005.0023

Leib, B. G., Jabro, J. D., & Matthews, G. R. (2003). Field evaluation and performance comparison of soil moisture sensors. *Soil Sci., 168*(6), 396-408. https://doi.org/10.1097/01.ss.0000075285.87447.86

Lo, T., Heeren, D. M., Mateos, L., Luck, J. D., Martin, D. L., Miller, K. A.,... Shaver, T. M. (2017). Field characterization of field capacity and root zone available water capacity for variable rate irrigation. *Appl. Eng. Agric., 33*(4), 559-572. https://doi.org/10.13031/aea.11963

Lo, T., Rudnick, D. R., Singh, J., Nakabuye, H. N., Katimbo, A., Heeren, D. M., & Ge, Y. (2020). Field assessment of interreplicate variability from eight electromagnetic soil moisture sensors. *Agric. Water Manag., 231,* 105984. https://doi.org/10.1016/j.agwat.2019.105984

Logsdon, S. D. (2009). CS616 Calibration: Field versus Laboratory. *SSSAJ, 73*(1), 1-6. https://doi.org/10.2136/sssaj2008.0146

McCann, I. R., Kincaid, D. C., & Wang, D. (1992). Operational characteristics of the Watermark Model 200 soil water potential sensor for irrigation management. *Appl. Eng. Agric., 8*(5), 603-609. https://doi.org/10.13031/2013.26131

Pringle III, H. C., Falconer, L. L., Fisher, D. K., & Krutz, L. J. (2019). Soybean irrigation initiation in Mississippi: Yield, soil moisture, and economic response. *Appl. Eng. Agric., 35*(1), 39-50. https://doi.org/10.13031/aea.12883

Rosenbaum, U., Huisman, J. A., Weuthen, A., Vereecken, H., & Bogena, H. R. (2010). Sensor-to-sensor variability of the ECH2O EC-5, TE, and 5TE sensors in dielectric liquids. *Vadose Zone J., 9*(1), 181-186. https://doi.org/10.2136/vzj2009.0036

Rothe, A., Weis, W., Kreutzer, K., Matthies, D., Hess, U., & Ansorge, B. (1997). Changes in soil structure caused by the installation of time domain reflectometry probes and their influence on the measurement of soil moisture. *Water Resour. Res., 33*(7), 1585-1593. https://doi.org/10.1029/97wr00677

Rudnick, D. R., Djaman, K., & Irmak, S. (2015). Performance analysis of capacitance and electrical resistance-type soil moisture sensors in a silt loam soil. *Trans. ASABE, 58*(3), 649-665. https://doi.org/10.13031/trans.58.10761

Saddiq, M. H., Wierenga, P. J., Hendrickx, J. M., & Hussain, M. Y. (1985). Spatial variability of soil water tension in an irrigated soil. *Soil Sci., 140*(2), 126-132. https://doi.org/10.1097/00010694-198508000-00008

Sadras, V. O., & Milroy, S. P. (1996). Soil-water thresholds for the responses of leaf expansion and gas exchange: A review. *Field Crops Res., 47*(2), 253-266. https://doi.org/10.1016/0378-4290(96)00014-7

Scanlon, B. R., Andraski, B. J., & Bilskie, J. R. (2002). Miscellaneous methods for measuring matric or water potential. In J. H. Dane, & C. G. Topp (Eds.), *Methods of soil analysis:* Part 4 physical methods (pp. 643-670). Madison, WI: SSSA. https://doi.org/10.2136/sssabookser5.4.c23

Schmitz, M., & Sourell, H. (2000). Variability in soil moisture measurements. *Irrig. Sci., 19*(3), 147-151. https://doi.org/10.1007/s002710000015

Shock, C. C., Barnum, J. M., & Seddigh, M. (1998). Calibration of Watermark soil moisture sensors for irrigation management. Proc. Irrigation Show & Education Conf. (pp. 139-146). Irrigation Association.

Singh, J., Lo, T., Rudnick, D. R., Irmak, S., & Blanco-Canqui, H. (2019). Quantifying and correcting for clay content effects on soil water measurement by reflectometers. *Agric. Water Manag., 216*, 390-399. https://doi.org/10.1016/j.agwat.2019.02.024

Soil Survey Staff. (2020). Web soil survey. Retrieved from https://websoilsurvey.sc.egov.usda.gov/

Spencer, G. D., Krutz, L. J., Falconer, L. L., Henry, W. B., Henry, C. G., Larson, E. J.,... Atwill, R. L. (2019). Irrigation water management technologies for furrow-irrigated corn that decrease water use and improve yield and on-farm profitability. *Crop Forage Turfgrass Manag., 5*(1). https://doi.org/10.2134/cftm2018.12.0100

Sui, R., Pringle III, H. C., & Barnes, E. M. (2019). Soil moisture sensor test with Mississippi Delta soils. *Trans. ASABE, 62*(2), 363-370. https://doi.org/10.13031/trans.12886

Thompson, R. B., Gallardo, M., Aguera, T., Valdez, L. C., & Fernandez, M. D. (2006). Evaluation of the Watermark sensor for use with drip irrigated vegetable crops. *Irrig. Sci., 24*(3), 185-202. https://doi.org/10.1007/s00271-005-0009-5

Thompson, R. B., Gallardo, M., Valdez, L. C., & Fernandez, M. D. (2007). Using plant water status to define threshold values for irrigation management of vegetable crops using soil moisture sensors. *Agric. Water Manag., 88*(1), 147-158. https://doi.org/10.1016/j.agwat.2006.10.007

Thomson, S. J., & Fletcher Armstrong, C. (1987). Calibration of the Watermark Model 200 soil moisture sensor. *Appl. Eng. Agric., 3*(2), 186-189. https://doi.org/10.13031/2013.26670

Thomson, S. J., Younos, T., & Wood, K. (1996). Evaluation of calibration equations and application methods for the Watermark granular matrix soil moisture sensor. *Appl. Eng. Agric., 12*(1), 99-103. https://doi.org/10.13031/2013.25444

Tollner, E. W., Tyson, A. W., & Beverly, R. B. (1991). Estimating the number of soil-water measurement stations required for irrigation decisions. *Appl. Eng. Agric., 7*(2), 198-204. https://doi.org/10.13031/2013.26211

Van Pelt, R. S., & Wierenga, P. J. (2001). Temporal stability of spatially measured soil matric potential probability density function. *SSSAJ, 65*(3), 668-677. https://doi.org/10.2136/sssaj2001.653668x

Varble, J. L., & Chavez, J. L. (2011). Performance evaluation and calibration of soil water content and potential sensors for agricultural soils in eastern Colorado. *Agric. Water Manag., 101*(1), 93-106. https://doi.org/10.1016/j.agwat.2011.09.007

Wilson, D. J., Western, A. W., & Grayson, R. B. (2004). Identifying and quantifying sources of variability in temporal and spatial soil moisture observations. *Water Resour. Res., 40*(2), W02507. https://doi.org/10.1029/2003wr002306